Int. J. Electrochem. Sci., 14 **(2019)** 8185 – 8194, doi: 10.20964/2019.08.12

International Journal of
ELECTROCHEMICAL
SCIENCE
www.electrochemsci.org

Short Communication

Effects of the Phosphorus Content in Ni-P substrate on Properties of Immersion Gold Coatings Obtained from Choline Chloride Solution

Yurong Wang[1], *Xiaoyun Cao*[2,3], *Zhiming Wang*[2,*], *Zhidong Chen*[3,*], *Naotoshi Mitsuzaki*[4]

[1] College of Pharmaceutical Science, Zhejiang Chinese Medical University, Hangzhou 310053, China
[2] School of Pharmaceutical and Chemical Engineering, Taizhou University, Taizhou 318000, China
[3] School of Petrochemical Engineering, Changzhou University, Changzhou 213164, China
[4] Qualtec Co., Ltd, Osaka 590-0906, Japan
[*]E-mail: zhiming@tzc.edu.cn, zdchen@cczu.edu.cn

Received: 1 April 2019 / *Accepted:* 20 May 2019 / *Published:* 30 June 2019

The effects of the phosphorus contents in electroless Ni-P substrates on the morphology, structure and corrosion resistance of gold coatings deposited on Ni-P surfaces, which were applied via a $HAuCl_4$-ChCl gold plating solution by galvanic displacement deposition, were investigated. Compared with low contents, high P content was not only more suitable to achieve bright golden Au surfaces, but also enabled the Ni-P coating to achieve high corrosion resistance during the immersion gold deposition process in the acidic gold plating solution and for further protection of the Cu sheet.

Keywords: Choline chloride; corrosion; electroless plating; phosphorus content

1. INTRODUCTION

Because of the superior properties of electroless nickel/immersion gold (ENIG) coatings, such as good electrical conductivity, excellent corrosion resistance, and good solderability [1-2], increasing attention has been paid to ENIG in electronic industries, especially for surface finishing or coatings for printed circuit boards (PCBs) to prevent the oxidation of the Ni-P coating deposited on the copper surface [3]. Traditionally, the gold coating on a Ni-P alloy substrate can be obtained from the potassium dicyanoaurate ($KAu(CN)_2$) solution due to its good bath stability and excellent performance [4]. Considering the toxicity of $KAu(CN)_2$ and the material compatibility problems, the application of this cyanide-containing procedure, however, has been gradually limited by governments worldwide[5]. Consequently, several non-cyanide baths have been developed for ENIG coatings, such as Au(I)-thiosulfate complex solutions and Au(I)-thiosulfate-sulfite mixed ligand solutions [6-7]. Recently, we

reported a simple and stable non-cyanide bath based on choline chloride (ChCl) and chloroauric acid ($HAuCl_4$) for immersion gold deposition onto electroless Ni-P substrates by a galvanic displacement process. The gold coating prepared from our ChCl solution has good properties for solderability and corrosion resistance [8].

The deposition of immersion gold on a Ni-P substrate can be considered a displacement reaction involving Ni atom oxidation and Au(I) cation reduction [9]. The ENIG process is often accompanied by excessive or uneven corrosion of the Ni-P substrate, and the hyperactive corrosion of the Ni-P layer during the immersion gold step has been known as a black spot or black pad defect, resulting in problems with joint integrity for wire bonding and soldering after assembly [10-13]. In the previous literature, it has been found that the corrosion resistance of as-deposited Ni-P alloys during the ENIG process greatly depends on the operating parameters, such as the substrate surface morphology or phosphor content, Au immersion time, coating bath temperature or pH value, and so on. [14-18].

As part of our ongoing study on the application of ChCl solutions to sustained electroless metal deposition [19-22], we chose the phosphor content of the Ni-P substrate as the most important parameter in our non-cyanide ChCl solution and investigated its effect on the ENIG process. Ni-P substrates with various phosphor contents from 6.5% to 10.5% were prepared, and the effects of the phosphor content on the surface morphology and properties of Au coatings were studied.

2. EXPERIMENTAL

2.1 Materials and methods

Copper (Cu) sheets (10 mm × 20 mm × 0.2 mm) were used as the substrates for ENIG deposition. All solutions were prepared with analytical grade reagents and distilled water.

The ENIG procedures are briefly described as follows. Cu sheets were treated in an alkali solution, acidic solution and activating solution to be degreased, micro-etched and activated, respectively. After each of these pretreatment steps, the substrates were rinsed with distilled water and dried under air flow. Then, pretreated Cu sheets were immersed in the Ni plating solution as described in Ref 23 [23] (22.4 g/L nickel sulfate, 25 g/L sodium hypophosphite, 21 mL/L lactic acid, 4 g/L DL-malic acid, 2 mg/L stabilizer, 8.5 g/L sodium acetate, 90 ℃) to obtain Ni-P coatings. Finally, the Ni-P plated Cu sheets were immersed in the Au(III)-ChCl plating solution (500 $g \cdot L^{-1}$ ChCl, 1.0 $g \cdot L^{-1}$ $HAuCl_4 \cdot 4H_2O$, pH 2.0, 80 ℃, 5 min) as detailed in our published work [8], performing immersion gold (IG) deposition to obtain 55 nm Au coatings.

2.2 Characterization

The structure and morphology of the coatings were investigated by X-ray diffraction (XRD, Rigaku D/max 2500 powder diffractometer, Cu Kα (λ=1.542 Å) radiation at 30 kV and 40 mA, a scan rate of 6 °·min^{-1}, 2θ from 30 ° to 80 °) and scanning electron microscopy (SEM, JSM-6360LA, Japan

Electron Optics Laboratory Co. Ltd., Japan), respectively. The phosphorus content of the Ni-P layer was detected by an Oxford Energy Dispersive X-ray Spectrometer (EDS) coupled to the SEM.

Electrochemical experiments were performed on an electrochemical workstation (RST-5200F, Suzhou Risetest Instrument Co. Ltd, Suzhou, China). Corrosion resistance was examined by the potentiodynamic polarization technique in 3.5 wt. % NaCl and 0.5 $mol \cdot L^{-1}$ solutions. Open circuit potential (OCP) tests were performed in the Au(III)-ChCl solution. The counter and reference electrodes were a platinum wire electrode and a saturated calomel electrode (SCE), respectively. The working electrodes for corrosion resistance and OCP tests were Ni-P/Au-coated and Ni-P-coated Cu sheets, respectively. The area of the working electrodes exposed to the solution was $1cm^2$, and the scan rate was 0.5 $mV \cdot s^{-1}$.

3. RESULTS AND DISCUSSION

3.1 Characterization of Ni-P coating with various phosphorus contents

Małecki et al. [24] revealed that the pH could influence the deposition rate of the electroless nickel (EN) plating and the P content in Ni-P coatings. Antonelli et.al.[25] also reported that the P deposition rate increased with decreasing pH. According to the above reports, different P contents in Ni-P coatings could be achieved simply by controlling the pH value of the EG plating solution.

Here, different P contents in the Ni-P coating were prepared by varying the pH value of the EG plating solution from 3.8 to 6.8 with ammonium hydroxide (NH_4OH) [23]. To establish the P content as the only factor influencing the Au coating, the thickness of the Ni-P coatings was controlled to be 3 μm by adjusting the electroless plating time [25]. The corresponding P contents in Ni-P coatings from various pH values and deposition times are shown in Table 1.

Table 1. P contents in Ni-P coatings from different pH values and deposition times.

pH	Time / min	P content / %
6.8	9	6.5
5.8	15	7.0
4.8	20	8.0
3.8	60	10.5

3.2 The effects of P content on the surface morphology of Au coatings

The results showed that the Au coating became dark and black with a decrease in the P content, which suggested that the Ni-P substrate with a low P content suffered serious corrosion during the gold plating process. Fig. 1 shows the surface morphologies of uncoated Ni-P substrates (inserts) and Au coatings with different P contents. It can be seen that the various P contents exhibited less of an influence on the Ni-P coatings and a greater influence on the Au coatings. The Au coating was smooth and golden when the P content was greater than 8.0 %, while it was covered with crevices and became dark when

the P content was less than 7.0 %. Elsener et al. [26] revealed that P-enriched Ni-P coatings have outstanding corrosion resistance, which could be explained by a strong enrichment of elemental P at the interface that limits the dissolution of Ni. Thus, Ni-P coatings with different P contents would dissolve in the strongly acidic Au plating solution to varying degrees during Au plating. Dissolution of Ni would lead to the formation of crevices [27].

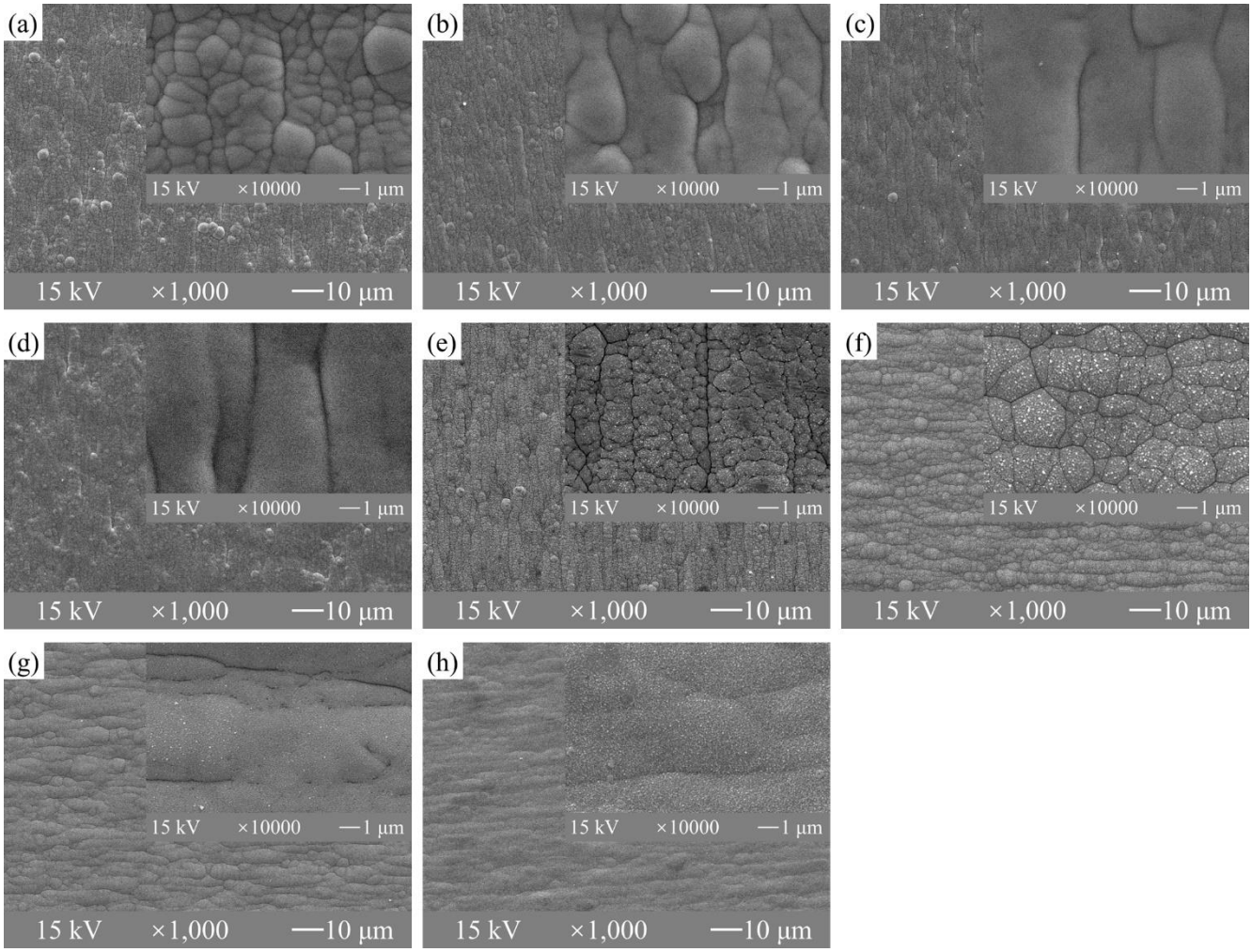

Figure 1. SEM images of Ni-P/Cu substrates with different levels of P contents (a-d) and Au coatings on Ni-P substrates (e-f). P content: (a,e) 6.5%, (b,f) 7.0%, (c,g) 8.0%, and (d,h) 10.5%. The conditions are as described in section 2.1 Materials and methods.

The components of Au coatings deposited on Ni-P substrates with different P contents were investigated through XRD. As shown in Fig. 2, an apparent peak located at 38.24° was ascribed to the Au (111) plane parallel to the surface of the substrate. The other diffraction peaks, Au (200) at 44.36° and Au (220) at 64.8°, exhibited extremely weak intensities compared to the Au (111) peak. These peaks in the XRD diagram were consistent with elemental Au diffractions (JCPDS 04-0784). Comparing each peak, there was no significant difference with the change in P content in the Ni layers. Additionally,

these observations also indicated that the preferential growth orientation was the Au (111) plane during the Au film formation process.

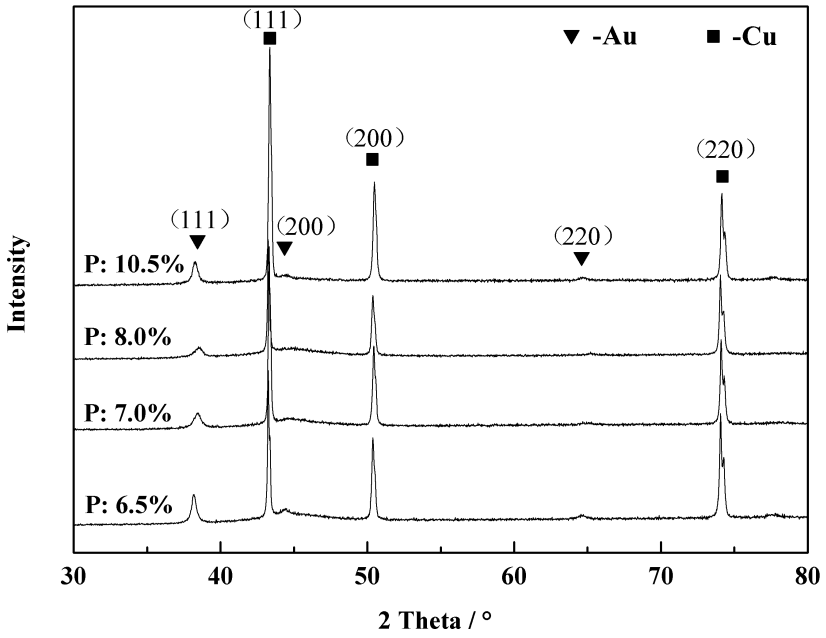

Figure 2. XRD patterns of Au coatings on Ni-P substrates with different P contents. The conditions are as described in section 2.1 Materials and methods.

3.3 The effects of the P content on the corrosion resistance of Ni-P/Au coatings

Potentiodynamic polarization measurements are widely used to study the corrosion resistance of deposited coatings [28]. Fig. 3 illustrates the potentiodynamic polarization curves of Ni-P coatings and Ni-P/Au coatings in 3.5 wt. % NaCl and 0.5 mol·L^{-1} H_2SO_4 solutions at room temperature. The electrochemical data extracted from the polarization curves, such as the corrosion potential (E_{corr}) and the corrosion current density (i_{corr}), are summarized in Table 2. Additionally, the polarization resistance (R_p) was calculated according to $R_p = \beta_a \times \beta_b \times 10^6 / [2.3 \times i_{coor} \times (\beta_a + \beta_b)]$ (β_a is the anodic Tafel slope, and β_c is the cathodic Tafel slope) [7,29] and the corresponding data are also listed in Table 2.

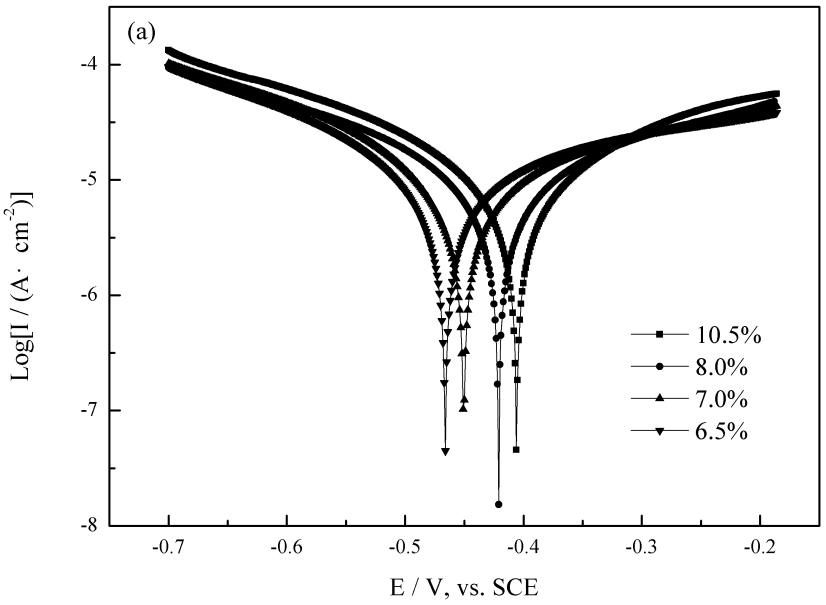
(a)
Log[I / (A· cm-2)]
E / V, vs. SCE
10.5%
8.0%
7.0%
6.5%

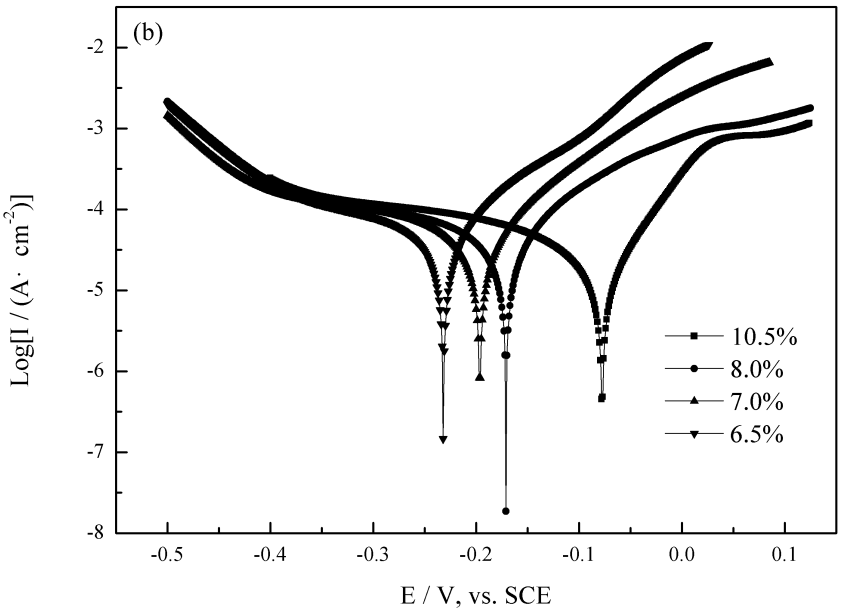
(b)
Log[I / (A· cm-2)]
E / V, vs. SCE
10.5%
8.0%
7.0%
6.5%

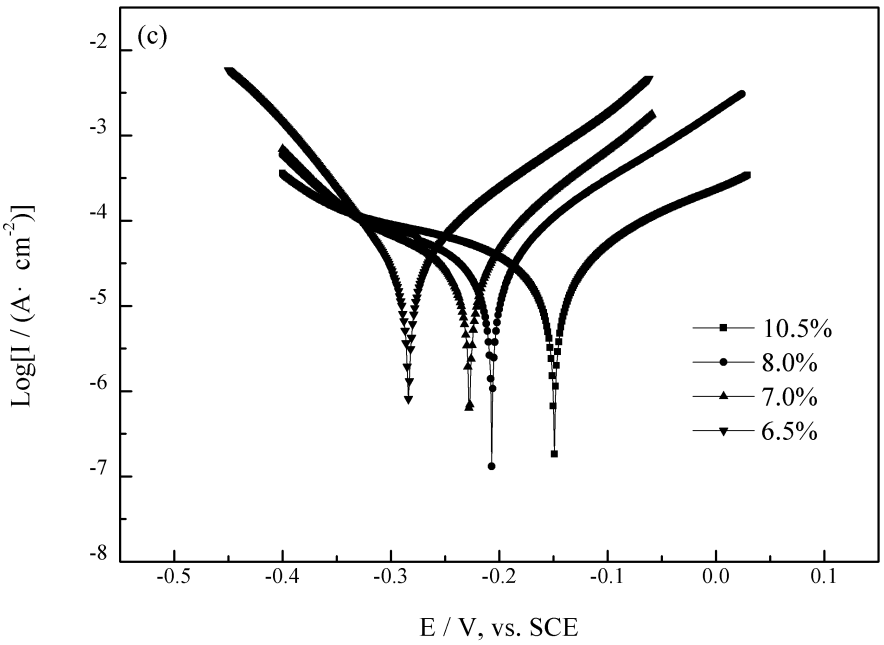

Figure 3. The potentiodynamic polarization curves of the Ni-P coatings with different P contents in (a) 3.5 wt. % NaCl and (b) 0.5 mol·L^{-1} H_2SO_4 and (c) the Ni-P/Au coatings with different P contents in 5 wt. % H_2SO_4 solutions.

Table 2. Electrochemical data extracted from the potentiodynamic polarization curves

P wt.%	E_{corr} (V)			i_{corr} (μA·cm^{-2})			Rp (Ω·cm^{-2})		
	a	b	c	a	b	c	a	b	c
6.5	-0.462	-0.230	-0.292	5.63	41.10	24.38	5790	663	649
7.0	-0.444	-0.192	-0.224	4.38	39.81	24.14	6358	742	915
8.0	-0.423	-0.176	-0.207	4.55	37.70	23.14	6407	890	1072
10.5	-0.406	-0.066	-0.143	5.05	20.15	19.46	6440	963	1467

It should be noted from Fig. 3 (a), 3 (b) and Table 2 that E_{corr} of the Ni-P coatings shifted positively, i_{corr} decreased, and R_p increased, with an increase in the P content both in NaCl solution and H_2SO_4 solution. Another phenomenon that was observed was that the difference in E_{corr} between the maximum and the minimum P content (ΔE_{corr}) was greater in H_2SO_4 solution (0.164 V) than in NaCl solution (0.056 V), and the R_p of the Ni-P coatings was higher in NaCl solution than in H_2SO_4 solution. These results indicated that Ni-P coatings with a lower P content had weaker corrosion resistance in acidic solution than in neutral solution. Bakhit et al. have revealed that the performance of nanocomposite coatings in a corrosive medium can be linked to four major aspects: the electrodeposition process, matrix properties, factors related to reinforcing particles, and service conditions [28]. Thus, with different P contents in the Ni-P layer, Ni and P developed into different crystal forms. Normally, the crystal structure of the Ni-P coating is amorphous at a higher-P content, while at a lower-P content, the Ni-P coating is crystalline [30]. The amorphous structure has a better corrosion resistance than the crystalline structure. Therefore, the corrosion resistance was enhanced by increasing the P content.

Because the Ni-P coating with different P contents showed a great difference in the acidic solution and because the pH value of our Au(III)-ChCl plating solution was 2.0, the potentiodynamic polarization curves of the Ni-P/Au coatings were obtained in H_2SO_4 solution to determine the influence of the P content on the Au coatings. As shown in Fig. 3 (b) and Fig. 3 (c), the E_{corr} of all the Ni-P/Au coatings was more negative than that of the corresponding Ni-P coatings. A possible reason for this result may be that the Ni-P coatings with different P contents were corroded during the ENIG Au deposition with an acid Au(III)-ChCl plating solution. As shown in Fig. 3 (c) and Table 2, E_{corr} of the Ni-P/Au coatings shifted positively, i_{corr} decreased, and R_p increased with increasing P content. The lower corrosion resistance with the lower P content could be ascribed to the fact that the surface of Ni-P/Au coatings with a low P content held cracks (as was seen in Fig. 1), where corrosion cells were easily formed to weaken the corrosion resistance [12,31]. As shown in Table 2, the i_{corr} and R_p of the Ni-P/Au coatings were lower and higher, respectively, than those of the corresponding Ni-P substrates. The lower i_{corr} of the Ni-P/Au coating indicated a lower corrosion rate of the Ni-P/Au coating than that of the Ni-P coating when the coating was corroded. Thus, Au can effectively decrease the corrosion rate of the Ni-P coating.

3.4 Open circuit potential of Ni-P substrates in Au plating solution

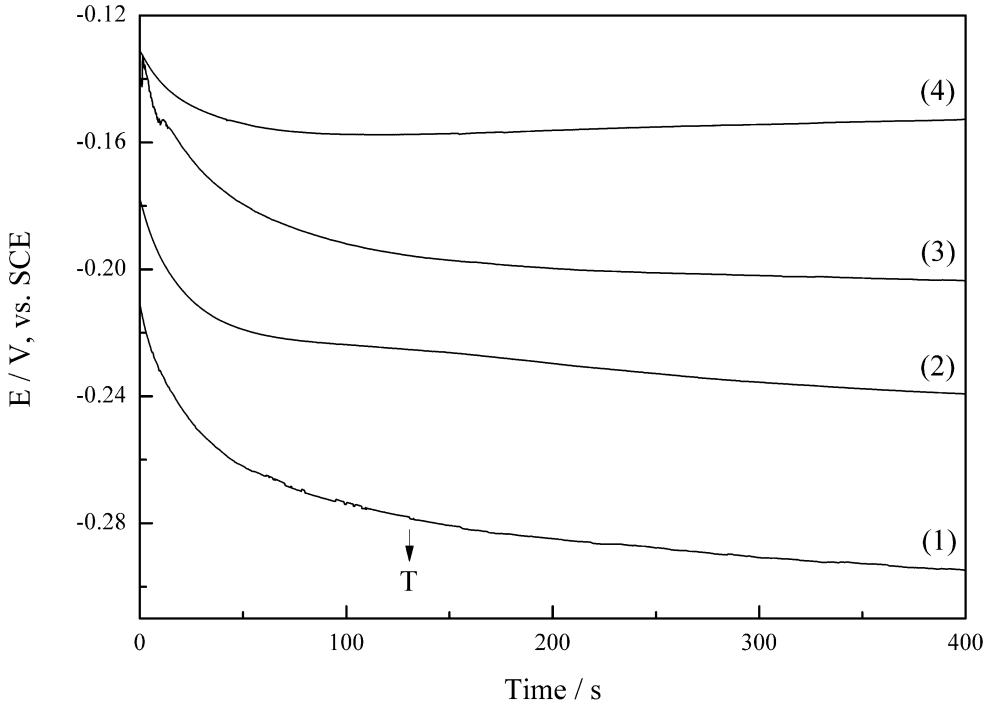

Figure 4. Ocp-t curves of Ni-P substrates with different P contents in Au plating solution. (1) 6.5%; (2) 7.0%; (3) 8.0% ; (4) 10.5%.

As Wang et al. revealed that the variations in open circuit potential during the IG process could reflect the changes of the coating surface state [7], the open circuit potential change versus time (OCP-

t) curves of Ni-P substrates with different P contents were tested in the Au plating solution. As shown in Fig. 4 and Table 3, the open circuit potentials (E_{OCP}) shifted negatively from the initial potential for all the Ni-P substrates, and with an increase in the P content from 6.5% to 10.5%, the plateau potential shifted to the positive direction, which indicates that gold film has an increased coverage on the Ni-P substrates. Moreover, the time for the potential to reach the plateau value corresponding to the time for the formation of Au coating on the Ni-P substrates became shorter. As shown in Table 3, the drops of the potential (ΔE) decreased with the increasing P contents. Thus, more extensive coverage with less time indicates that Ni-P coating with high P content leads to a uniform and compact Au coating, which could provide better protection for Ni substrate.

Table 3. Electrochemical data extracted from the open circuit potential-time curves

P content / %	Initial potential / mV	Plateau potential / mV	ΔE / mV
6.5	-211	-294	83
7	-177	-249	64
8	-141	-202	61
10.5	-131	-153	22

4. CONCLUSIONS

The SEM figures indicated that the surface of the coating with a low P content is covered with cracks, this was caused by the corrosion of the Ni-P coating in the strongly acidic gold plating solution. Higher P contents in the Ni-P coating enable a better corrosion resistance under acidic conditions. Therefore, a Ni substrate with a high P content should be chosen for the IG process in a strongly acidic gold plating system.

ACKNOWLEDGMENTS
The authors greatly acknowledge the financial support from the National Natural Science Foundation of China (Grant No. 51401038, 51574047).

References

1. S. Siau, A. Vervaet, L. Degrendele, J. D. Baets and A. V. Calster, *Appl Surf Sci*., 252 (2006) 2717.
2. S. Gao, Z. Chen, A. Hu, M. Li and K. Qian, *J Mater Process Tech*., 214 (2014) 326.
3. R. K. Sharma, R. Kaneriya, S. Patel, A. Bindal and K. C. Pargaien, *Microelectron Eng*., 108 (2013) 45.
4. T. N .Vorobyova, S. K. Poznyak, A. A. Rimskaya and O. N. Vrublevskaya, *Surf Coat Technol*., 176 (2004) 327.
5. M. Kato, J. Sato, H. Otani, T. Homma, Y. Okinaka, T. Osaka and O. Yoshioka, *J Electrochem Soc*., 149(3) (2002) C164.
6. J. Sato, M. Kato, H. Otani, T. Homma, Y. Okinaka, T. Osaka and O. Yoshioka, *J Electrochem Soc.*, 149(3) (2002) C168-C172.
7. Y. Wang, H. Liu, S. Bi, M. He, C. Wang and L. Cao, *RSC Adv.*, 6 (2016) 9656.

8. Y. Wang, X. Cao, W. Wang, N. Matsuzaki and Z. Chen, *Surf Coat Technol*., 265 (2015) 62.
9. R. J. Coyle, D. E. H. Popps, A. Mawer, D. P. Cullen, G. M. Wenger and P. P. Solan, *IEEE Trans Compon Packag Technol*., 26(3) (2003) 724.
10. R. Ramanauskas, A. Selskis, J. Juodkazyte and V. Jasulaitiene, *Circuit World*, 39(3) (2013) 124.
11. D. J. Lee and H. S. Lee, *Microelectron Reliab*., 46 (2006) 1119.
12. Y. S. Won, S. S. Park, J. Lee, J. Y. Kim and S. J. Lee, *Appl Surf Sci.*, 257 (2010) 56.
13. K. H. Kim, J. Yua and J. H. Kim, *Scripta Mater*., 63 (2010) 508.
14. T. S. N. Sankara Narayanan, I. Baskaran, K. Krishnaveni and S. Parthiban, *Surf Coat Technol*., 2006 (2006) 3438.
15. G. Cui, J. Zhao, S. Liu and G. Wu, *J Phys Chem C*, 115 (2011) 21169.
16. A. D. Ballantyne, G. C. H. Forrest, G. Frisch, J. M. Hartley and K. S. Ryder, *Phys Chem Chem Phys.*, 17 (2015) 30540.
17. Q. V. Bui, J. W. Yoon and S. B. Jung, *J Nanosci Nanotechnol.*, 12 (2012) 3506.
18. H. Liu, A. Mao, M. He, Y. Wang, S. Bi, C. Wang and L. Cao, *Int J Electrochem Sci*,. 10 (2015) 7811.
19. Y. Wang, C. Yang, J. He, W. Wang, N. Matsuzaki and Z. Chen, *Appl Surf Sci*., 372 (2016) 1.
20. Y. Wang, W. Li, W. Wang, N. Matsuzaki, W. Bao and Z. Chen, *Thin Solid Films*, 586 (2105) 35.
21. Y. Wang, J. He, W. Wang, M. Naotoshi and Z. Chen, *J Electrochem Soc*., 160(8) (2013) D295.
22. Y. Wang, Y. Zhou, W. Wang and Z. Chen, *J Electrochem Soc*., 160(3) (2013) D119.
23. B. H. Chen, L. Hong, Y. Ma and T. M. Ko, *Ind Eng Chem Res*., 41 (2002) 2668.
24. A. Małecki and A. Micek-Ilnicka, *Surf Coat Tech.*, 123 (2000) 72.
25. S. B. Antonelli, T. L. Allen, D. C. Johnson and V. M. Dubin, *J Electrochem Soc*., 152(9) (2005) J120.
26. E. Bernhard, C. Maura, A. S. Mariano and R. Antonella, *J Appl Electrochem*., 38 (2008) 1053.
27. K. Zeng, R. Stierman, D. Abbott and M. Murtuza, *JOM*., 58(6) (2006) 75.
28. B. Bakhit, A. Akbari, F. Nasipouri and M. G. Hosseini, *Appl Surf Sci*., 307 (2014) 351.
29. Y. Wang, R. Tang, C. Yang, T. Xu, N. Mitsuzaki and Z. Chen, *Thin Solid Films*, 669 (2019) 72.
30. M. O. Alam and Y. C. Chan, *J Appl Phys.*, 94(6) (2003) 4108.
31. C. Gu, J. Lian, J. He, Z. Jiang and Q. Jiang, *Surf Coat Technol.*, 200 (2006) 5413.